

# Quantum Theory of Transmission Line Resonator-Assisted Cooling of a Micromechanical Resonator

Yong Li,<sup>1</sup> Ying-Dan Wang,<sup>1,2</sup> Fei Xue,<sup>3,4,5</sup> and C. Bruder<sup>1</sup>

<sup>1</sup>*Department of Physics, University of Basel, Klingelbergstrasse 82, 4056 Basel, Switzerland*

<sup>2</sup>*NTT Basic Research Laboratories, NTT Corporation, Atsugi-shi, Kanagawa 243-0198, Japan*

<sup>3</sup>*CREST, Japan Science and Technology Agency (JST), Kawaguchi, Saitama 332-0012, Japan*

<sup>4</sup>*Frontier Research System, The Institute of Physical and Chemical Research (RIKEN), Wako-shi, Saitama 351-0198, Japan*

<sup>5</sup>*Department of Electrical Engineering, Technion, Haifa 32000, Israel*

(Dated: September 13, 2008)

We propose a quantum description of the cooling of a micromechanical flexural oscillator by a one-dimensional transmission line resonator via a force that resembles cavity radiation pressure. The mechanical oscillator is capacitively coupled to the central conductor of the transmission line resonator. At the optimal point, the micromechanical oscillator can be cooled close to the ground state, and the cooling can be measured by homodyne detection of the output microwave signal.

PACS numbers: 85.85.+j, 45.80.+r, 03.67.Mn, 42.50.Lc

## I. INTRODUCTION

Micro- and nano-mechanical resonators have been an interesting research topic due to their broad application in technology and fundamental physics [1]. This includes studies of ultrahigh precision displacement detection [2], mass detection [3], gravitational-wave detectors [4, 5], and attempts to observe quantum behavior of mechanical motion [6–10]. Many of the applications are fundamentally limited by thermal fluctuations, and in order to reduce their effects, it is desirable to cool the mechanical oscillators. Recently, various schemes like the laser sideband cooling schemes developed for trapped ions and atoms [11], have been proposed for significantly cooling a mechanical resonator (MR) coupled to a Cooper-pair box [12–15], a flux qubit [16, 17], a superconducting single-electron transistor [18], quantum dots [19], trapped ions [20], and optical cavities [21–39]. On the experimental side, optomechanical cooling schemes have been shown to be promising [21–28]: the MR was cooled to ultralow temperatures via either photothermal forces or radiation pressure by coupling it to a driven cavity. There are two main optomechanical cooling schemes. The first one involves an active feedback loop [24, 29, 30], and the second one works via passive back-action cooling (also called self-cooling) [22, 23, 25, 26]. A fully quantum-mechanical description of cavity-assisted cooling schemes for optomechanical systems has been given in Refs. [32–37] (for a review, see [38, 39]). Ground-state cooling of a mechanical resonator via passive cooling schemes based on radiation pressure has also been investigated theoretically [33, 34, 36, 37].

Recently, other optomechanical-like cooling schemes have been proposed to replace the optical cavity by a radio-frequency (RF) circuit [40, 41] or a one-dimensional transmission line resonator (TLR) [42]. However, the theoretical understanding of the cooling schemes via a RF circuit in Refs. [40, 41] or via a TLR in Ref. [42] is based on a classical description of the motion of the

MR. A quantum-mechanical description of the motion of the MR, in a similar system consisting of a mechanical resonator capacitively coupled to a superconducting coplanar waveguide (which is an example of a TLR), was discussed recently in Ref. [43], which focused on studying the entanglement between the MR and the TLR without considering the cooling of MR. Most recently, Teufel *et al.* [44] considered the cooling of a MR by applying directly the theoretical analysis of the cavity-assisted back-action cooling scheme [34] to a superconducting microwave resonator. They also presented experimental data about the cooling effect on the MR due to the microwave radiation field. The quantum-mechanical description of TLR-assisted cooling of a MR has also been investigated in Ref. [45] via embedding a SQUID [46], which allows to control the coupling strength between MR and TLR by controlling the flux through the SQUID.

There are some practical advantages [47, 48] in the microwave TLR schemes. The TLR is realized in a thin on-chip superconducting film and is easily pre-cooled by standard dilution refrigeration techniques. It is ready to be integrated with quantum circuits containing Josephson junctions which may offer a sensitive measurement and a connection with quantum information processing. In addition, the size of the mechanical resonator could be much smaller than the wavelength of the radiation in the TLR, unlike in optical cavity experiments that work with reflection.

In this paper, we present a quantum-mechanical description and use it to investigate the motion of the MR when it is coupled capacitively to a driven TLR as in Ref. [42] where the calculation was carried out in a semi-classical framework. The Hamiltonian of our TLR-assisted model is also studied in Refs. [43, 44], and is very similar to that of a MR coupled to a driven optical cavity via radiation pressure coupling [32–39]. We study the TLR-assisted passive back-action cooling of a MR in detail by using a quantum Langevin description (without taking into account quantum entanglement [43] between the MR and the TLR). One of the main results

of our work is to show that the MR can be cooled close to its ground state using realistic parameters: final effective mean phonon numbers below 1 can be reached assuming an initial temperature of 10 mK which can be achieved using a dilution refrigerator. We discuss in detail how such a ground state cooling of the MR can be obtained for all kind of parameter choices in practice.

## II. MODEL AND HAMILTONIAN

The system that we consider is shown schematically in Fig. 1: a MR is fixed on both ends (or a cantilever fixed on one end) located at the center of the TLR and is coupled capacitively to the central conductor of the TLR [49]. We restrict the description to the fundamental flexural mode of oscillation of the MR which is modeled as a harmonic oscillator of frequency  $\omega_b$  and effective mass  $m$ . The TLR is driven by an external microwave at a frequency  $\omega_d$  and can be modeled as a single mode LC resonator with frequency  $\omega'_a = 1/\sqrt{L_a C_a}$  (the second mode of the TLR [50]), where  $L_a$  is the inductance and  $C_a$  the capacitance of the TLR.

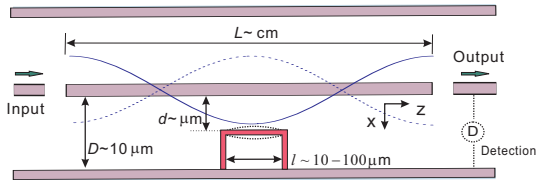


FIG. 1: (Color online) Schematic diagram of a mechanical resonator (MR) located at the center of a one-dimensional transmission-line resonator (TLR). The external microwave drive field enters from the left and drives the TLR. The signal at the output on the right end can be used to measure the motion of the MR via homodyne detection [32, 44, 47, 61].

The Hamiltonian of the system reads

$$H = \hbar\omega'_a a^\dagger a + \left( \frac{p^2}{2m} + \frac{m\omega_b^2}{2} x^2 \right) + \frac{C_g(x)}{2} V^2 + \hbar(\varepsilon a^\dagger e^{-i\omega_d t} + \varepsilon^* a e^{i\omega_d t}). \quad (1)$$

The first line describes the free Hamiltonian of the TLR and the MR, respectively, with lowering (rising) operator of the TLR mode  $a$  ( $a^\dagger$ ), and the position (momentum) operator of the MR  $x$  ( $p$ ) which satisfy  $[a, a^\dagger] = 1$  and  $[x, p] = i\hbar$ . The first term in the second line is the capacitive coupling between the TLR and the MR. Actually, it describes the capacitive energy between them. The MR and the TLR are assumed to form a capacitor with the capacitance  $C_g(x) \approx C_g^0(1 - x/d)$  (for small displacement) depending on the position of the MR along the  $x$ -direction ( $d$  is the initial equilibrium distance without the coupling and  $C_g^0$  the corresponding initial capacitance; typically  $d \sim 1 \mu\text{m}$  [47]). The capacitor is assumed

to be placed in the center of the structure, i.e., its voltage is given by the antinode voltage of the second mode:  $V = V_{rms}(a^\dagger + a)$  (where  $V_{rms} = \sqrt{\hbar\omega'_a/C_a}$  is the rms voltage [49]), since the length of the MR is usually much shorter than that of the TLR:  $L \sim \text{cm} \gg l \sim 10 - 100 \mu\text{m}$ . The last term in Eq. (1) describes the input driving of the TLR by an external microwave field with the coupling strength [22, 36, 49]  $|\varepsilon| = \sqrt{2\kappa P/\hbar\omega'_a}$ , where  $\kappa$  is the decay rate of the TLR,  $P$  is the input external microwave drive power. Here, the non-rotating wave terms like  $a e^{-i\omega_d t}$  and  $a^\dagger e^{i\omega_d t}$  have been ignored since we keep  $|\varepsilon| \ll \omega'_a \sim \omega_d$ .

Usually, the fundamental oscillation frequency is of the order of  $2\pi \times (10^3 - 10^6)$  Hz for micromechanical resonators and  $2\pi \times (10^7 - 10^9)$  Hz for nanomechanical resonators; the TLR frequency can be made to be of the order of  $2\pi \times 10$  GHz. Here we will focus on the case of a micro-MR for which the condition  $\omega_b \ll \omega'_a$  is satisfied. In the interaction picture with respect to  $\hbar\omega_d a^\dagger a$  and neglecting the rapidly-oscillating terms, the Hamiltonian reads

$$H_I = \hbar\Delta_0 a^\dagger a + \left( \frac{p^2}{2m} + \frac{m\omega_b^2}{2} x^2 \right) - \frac{\hbar g_0}{2} (2a^\dagger a + 1)x + \hbar(\varepsilon a^\dagger + \varepsilon^* a) \quad (2)$$

where  $g_0 := C_g^0 V_{rms}^2 / (\hbar d)$  is a real coupling constant;  $\Delta_0 = \omega_a - \omega_d$  is the detuning, and  $\omega_a = \omega'_a + C_g^0 V_{rms}^2 / \hbar$  is the modified frequency of the TLR shifted by the coupling between TLR and MR.

This Hamiltonian resembles that used in cavity-assisted cooling schemes [32-37]. This suggests that the capacitive-coupling scheme in a microwave TLR can be used to cool the MR like in the case of radiation-pressure cooling in an optical cavity.

## III. QUANTUM LANGEVIN EQUATIONS AND FINAL MEAN PHONON NUMBER

The dynamics is also determined by fluctuation-dissipation processes that affect both the TLR and the mechanical mode. They are taken into account in a fully consistent way by the quantum Langevin equations [51]:

$$\dot{x} = p/m, \quad (3a)$$

$$\dot{p} = -m\omega_b^2 x - \gamma_b p + \frac{\hbar g_0}{2} (2a^\dagger a + 1) + \xi, \quad (3b)$$

$$\dot{a} = -(\kappa + i\Delta_0)a + ig_0 a x + \varepsilon + \sqrt{2\kappa} a_{in}. \quad (3c)$$

Here  $a_{in}$  ( $a_{in}^\dagger$ ) is the noise operator due to the external microwave drive, and  $\xi(t)$  denotes the quantum Brownian

force that the resonator is subject to. They satisfy [51]

$$\langle a_{in}(t)a_{in}^\dagger(t') \rangle = (N+1)\delta(t-t'), \quad (4)$$

$$\langle \xi(t)\xi(t') \rangle = \frac{\hbar\gamma_b m}{2\pi} \int d\omega e^{-i\omega(t-t')} \omega \left(1 + \coth \frac{\hbar\omega}{2k_B T}\right), \quad (5)$$

where  $N = 1/[\exp(\hbar\omega_a/k_B T) - 1]$  is the mean number of thermal microwave photons of the TLR,  $k_B$  is the Boltzmann constant,  $T$  the temperature of the environment, and  $\gamma_b$  the damping rate of the MR. For simplicity, we have assumed that both the bath correlated to the external microwave drive field and the one connected to the MR have the same temperature [43]. We now perform a similar calculation as that given in Refs. [32, 36, 37, 52]. The steady-state solution of the quantum Langevin equations (3) can be obtained by first replacing the operators by their average and then setting  $d(\dots)/dt = 0$ . Hence we can get the steady-state values as

$$\langle p \rangle = 0, \quad \langle x \rangle = \frac{\hbar g_0 \left( |\langle a \rangle|^2 + \frac{1}{2} \right)}{m\omega_b^2}, \quad \langle a \rangle = \frac{\varepsilon}{\kappa + i\Delta}, \quad (6)$$

where  $\Delta = \Delta_0 - g_0 \langle x \rangle$  is the effective detuning. In Eq. (6), we can also take  $|\langle a \rangle|^2 + \frac{1}{2} \simeq |\langle a \rangle|^2$ , since we will focus on the case  $|\langle a \rangle| \gg 1$  which can be achieved by controlling the input power of the external microwave drive.

Rewriting each operator as a  $c$ -number steady-state value plus an additional fluctuation operator, and neglecting the nonlinear terms (since we have chosen  $|\langle a \rangle| \gg 1$ ), we obtain a set of linear quantum Langevin equations (see Eq. (A1)) and then solve for the spectrum of the position and momentum of the MR as in Refs. [32, 36, 37, 52], see Appendix A.

Using the fluctuation spectra of the MR as given in Eqs. (A10,A11), we can define the final mean phonon number in the steady state [36] as

$$n_b^f = \frac{\langle \delta p^2 \rangle}{2\hbar m \omega_b} + \frac{m\omega_b}{2\hbar} \langle \delta x^2 \rangle - \frac{1}{2}, \quad (7)$$

where the variances of position and momentum are

$$\langle \delta r^2 \rangle = \frac{1}{2\pi} \int_{-\infty}^{+\infty} S_r(\omega) d\omega, \quad (r = x, p). \quad (8)$$

This allows us to define the effective temperature  $T_{\text{eff}}$  as

$$T_{\text{eff}} = \frac{\hbar\omega_b}{k_B} \ln^{-1} \left( \frac{1}{n_b^f} + 1 \right). \quad (9)$$

In the next section, we will consider the cooling of the MR by discussing its final effective mean phonon number (or equivalently, its effective temperature) in detail.

#### IV. COOLING OF THE MR

The final effective mean phonon number of the MR can be calculated directly by evaluating the integral in Eq. (8) numerically and using Eq. (7). Alternatively, instead of being evaluated directly, Eq. (8) can also be evaluated analytically using the approximation scheme described in the following.

The effective mechanical damping rate  $\gamma_b^{\text{eff}}(\omega) = \gamma_b + \gamma_{ca}(\omega)$  can be significantly increased,  $|\gamma_b^{\text{eff}}(\omega)| \gg \gamma_b$ , when  $|g_0 \langle a \rangle|$  is very large, see Eq. (A16). Let us consider the most interesting regime when the significantly increased effective mechanical damping rate is less than the mechanical frequency:  $|\gamma_b^{\text{eff}}(\omega)| < \omega_b$ , (that is, the effective quality factor  $Q_b^{\text{eff}} = \omega_b/|\gamma_b^{\text{eff}}(\omega)| > 1$ ), and also less than the decay rate of TLR:  $|\gamma_b^{\text{eff}}(\omega)| < \kappa$  [33, 34, 37, 53]. In this regime, the effective frequency is unchanged  $\omega_b^{\text{eff}}(\omega) \simeq \omega_b$  [36, 54] according to Eq. (A15), and the effective susceptibility is peaked around the points  $\omega = \pm \omega_b^{\text{eff}}(\omega) \simeq \pm \omega_b$ . Then one can get an approximate expression for the variance

$$\langle \delta x^2 \rangle \approx \frac{S'_{th}(\omega_b) + S'_{ca}(\omega_b)}{2m^2\omega_b^2 |\gamma_b^{\text{eff}}(\omega_b)|}, \quad (10)$$

where the effective thermal noise spectrum  $S'_{th}(\omega)$  and the induced noise spectrum  $S'_{ca}(\omega)$  are the symmetrized parts of  $S_{th}(\omega)$  and  $S_{ca}(\omega)$ , respectively:

$$S'_{th}(\omega) = \hbar\gamma_b m \omega \coth \frac{\hbar\omega}{2k_B T}, \quad (11)$$

$$S'_{ca}(\omega) = (2N+1) \hbar m \frac{\kappa^2 + \Delta^2 + \omega^2}{2\Delta} \gamma_{ca}(\omega). \quad (12)$$

Similarly, one can obtain

$$\langle \delta p^2 \rangle = (m\omega_b)^2 \langle \delta x^2 \rangle. \quad (13)$$

Figure 2 shows the variance of position  $\langle \delta x^2 \rangle$  as a function of the effective detuning  $\Delta$ . The dashed lines correspond to a numerical evaluation of the integral in Eq. (8). The solid lines describe the approximate results obtained through Eq. (10) which can be seen to agree perfectly with the exact numerical evaluation. We checked that this is also the case for the variance of the momentum  $\langle \delta p^2 \rangle$ .

In Eq. (10), the induced noise spectrum  $S'_{ca}(\omega_b)$  increases (heats) the motion of the MR. On the other hand, when the effective damping rate is enhanced:  $|\gamma_b^{\text{eff}}(\omega_b)| > \gamma_b$ , the mechanical motion will reduce, that means cooling. Mathematically, the cooling effect would dominate the heating effect when the effective damping rate is sufficiently increased. Actually, this is right when the significantly increased effective damping rate is positive for positive detuning. However, it is not the case when  $\gamma_b^{\text{eff}}(\omega_b)$  is negative and  $|\gamma_b^{\text{eff}}(\omega_b)| \gg \gamma_b$  (for negative detuning  $\Delta < 0$ ). That is because the stability conditions, derived using Ref. [55], are satisfied only for positive detuning

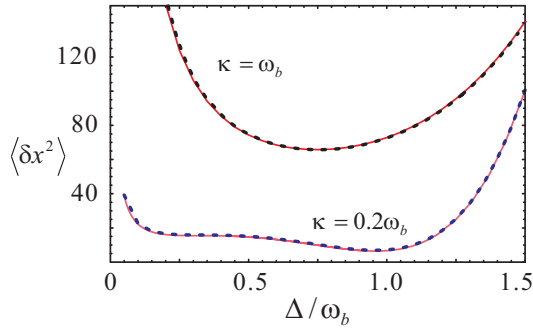


FIG. 2: (Color online) Variance of position  $\langle \delta x^2 \rangle$  in units of  $\hbar/m\omega_b$  as a function of effective detuning  $\Delta$ . The dashed lines are obtained by numerically evaluating the integral in Eq. (8), the solid lines by using the approximate expressions Eqs. (10,13). Here,  $T = 6 \times 10^3 \hbar\omega_b/k_B$ ,  $g_0 = 3 \times 10^{-5} \omega_b \sqrt{m\omega_b/\hbar}$ ,  $\omega_a = 2 \times 10^4 \omega_b$ ,  $\varepsilon = 2.5 \times 10^3 \omega_b$ ,  $\gamma_b = 0.25 \times 10^{-4} \omega_b$ , and  $\kappa = \omega_b$  (upper lines) or  $\kappa = 0.2\omega_b$  (lower lines).

[32, 52, 60]. In fact, a negative effective damping means the amplitude motion of the MR will be amplified which will lead to an instability [56–58].

In what follows, we will focus on the case of positive detuning  $\Delta > 0$ . According to Eqs. (7,10,13), one has

$$n_b^f = \frac{\gamma_b n_b + \gamma_{ca}(\omega_b) n_{ca}}{\gamma_b + \gamma_{ca}(\omega_b)}, \quad (14)$$

where

$$n_b \equiv \frac{S'_{th}(\omega_b)}{2\hbar m \gamma_b \omega_b} - \frac{1}{2} \equiv \frac{1}{\exp(\hbar\omega_b/k_B T) - 1} \quad (15)$$

is the initial mean thermal excitation phonon number of the MR;

$$n_{ca} \equiv \frac{2N + 1}{4\omega_b \Delta} (\kappa^2 + \Delta^2 + \omega_b^2) - \frac{1}{2} \quad (16)$$

is the induced mean phonon number due to the capacitive coupling between the MR and the TLR.

As discussed above, the significant reduced value of  $n_b^f$  in Eq. (14) can only be obtained when the additional damping rate  $\gamma_{ca}(\omega_b)$  (or effective damping rate  $\gamma_b^{\text{eff}}(\omega_b)$ ) is positive and much larger than the original one (but still less than the decay rate of TLR and less than the frequency of the MR as discussed before):

$$\gamma_b \ll \gamma_{ca}(\omega_b) < (\omega_b, \kappa). \quad (17)$$

This can be satisfied by enhancing the value of  $|g_0 \langle a \rangle|$ , that is, by controlling the capacitive coupling strength  $g_0$  and increasing the external microwave drive power  $P$  to make  $|\varepsilon|$  large (equivalently,  $|\langle a \rangle|$  will be large). In practice, the capacitive coupling strength  $g_0$  would be limited by the realistic system, and the external microwave drive strength  $\varepsilon$  would also be limited according to the validity of the rotating wave approach as we mentioned before.

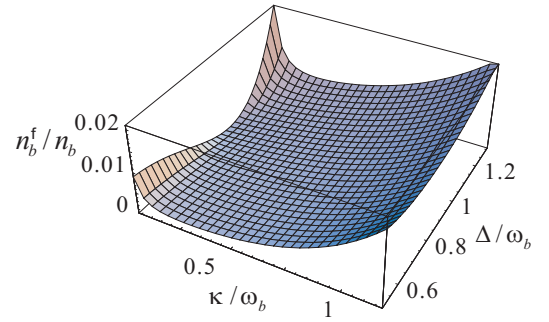


FIG. 3: (Color online) Final mean phonon number in the steady state  $n_b^f$  vs. effective detuning  $\Delta$  and decay rate  $\kappa$  of the TLR ( $T = 3 \times 10^4 \hbar\omega_b/k_B$ , for the other parameters see Fig. 2).

Here we put the length of the MR  $l$  as large as 10 – 100  $\mu\text{m}$  and the distance between the MR and TLR  $d$  as small as 1  $\mu\text{m}$  (see Fig. 1) in order to get a large capacitance  $C_g^0$  which will lead to large  $g_0$ , and fix  $|\varepsilon| = \omega_a/8$  for all the numerical calculations. Then for a significantly-increased effective damping rate, the final mean phonon number reduces to

$$n_b^f = \frac{\gamma_b}{\gamma_{ca}(\omega_b)} n_b + n_{ca}. \quad (18)$$

In order to get the ground state cooling, that is,  $n_b^f \ll 1$ , both  $n_{ca}$  and  $n_b \gamma_b / \gamma_{ca}(\omega_b)$  should be much less than 1. Especially, if the  $\gamma_{ca}(\omega_b)$  is significantly increased enough to make

$$\gamma_b n_b \ll \gamma_{ca}(\omega_b) n_{ca}, \quad (19)$$

then  $n_b^f$  approaches the limit  $n_{ca}$ :

$$n_b^f \rightarrow n_{ca}. \quad (20)$$

Now we discuss the possible minimal value of  $n_{ca}$  by discussing all kinds of parameters, e.g.,  $\kappa$ ,  $\Delta$ , and  $N$ . From Eq. (16), it is obvious that the optimal value of  $\kappa$  satisfies the high-quality cavity limit

$$\kappa^2 \ll \omega_b^2, \quad (21)$$

and the optimal detuning satisfies  $\Delta = \sqrt{\omega_b^2 + \kappa^2} \approx \omega_b$ . Then the corresponding induced mean phonon number  $n_{ca}$  is

$$n_{ca} \approx N + \frac{\kappa^2}{4\omega_b^2}. \quad (22)$$

The optimal  $N$  needs a sufficiently low initial temperature of the bath which is limited in practice to the experimental dilute refrigerator temperatures. For the superconducting TLR scheme, its microwave frequency is of the order of  $2\pi \times 10^{10}$  Hz. For the initial temperature  $T \gtrsim 1$  K,  $k_B T \gtrsim \hbar\omega_a$  and  $N \gtrsim 1$ , the ground-state cooling of the MR is not possible. Therefore, initial

temperature less than 100 mK are required to achieve ground-state cooling.

Our result on the limiting value in Eq. (22) is consistent with that in other optical schemes except the limit of initial temperatures. In the optical cavity case  $\hbar\omega_a \gg k_B T$  (even at room temperature) and therefore  $N \simeq 0$ , the optimal value of  $n_{ca}$  becomes

$$n_{ca} \approx \frac{\kappa^2}{4\omega_b^2}, \quad (23)$$

which is just the case of resolved sideband cooling as discussed in the optomechanical cooling schemes [22, 23, 25, 26, 28]. We would like to point out that these references also mention another cooling limit: the Doppler cooling limit, which is realized in our system when  $N \simeq 0$ ,  $\Delta = \sqrt{\omega_b^2 + \kappa^2}$ , and  $\kappa^2 \gg \omega_b^2$  in Eq. (16):

$$n_{ca} \approx \frac{\kappa}{2\omega_b} > 1. \quad (24)$$

On the other hand, if  $N \gg \kappa^2/4\omega_b^2$ , the induced mean phonon number  $n_{ca}$  in Eq. (22) becomes  $n_{ca} \rightarrow N$ . In the classical limit when the initial temperature is so high that  $N \approx k_B T/(\hbar\omega_a) \gg 1$ , one has

$$\frac{T_{\text{eff}}}{T} = \frac{n_b^f}{n_b} \approx \frac{n_{ca}}{n_b} = \frac{\omega_a}{\omega_b}, \quad (25)$$

which is also given in Ref. [31]. The Doppler cooling limit in Eq. (24) and the classical cooling limit in Eq. (25) preclude ground state cooling. We will focus on the resolved sideband cooling in this paper.

The final mean phonon number  $n_b^f$  is plotted as a function of the effective detuning  $\Delta$  and the decay rate  $\kappa$  of the TLR in Fig. 3. It is clear that one can obtain a significant suppression of the mechanical motion of the MR in the positive detuning range  $\Delta \simeq \omega_b$ . The optimal cooling is obtained for  $\kappa^2 \ll \omega_b^2$ , which agrees with both the above analysis and that in other treatments of radiation-pressure cooling [22, 23, 25, 26, 42].

Physically, as discussed in the back-action optomechanical cooling schemes in optical cavities (Refs. [33, 34, 36, 37, 60]), the external driving microwave is scattered by the ‘‘TLR + MR’’ system mostly to the first Stokes sideband ( $\omega_d - \omega_b$ ) and the first anti-Stokes sideband ( $\omega_d + \omega_b$ ). The generation of an anti-Stokes photon will cool the MR by taking away a phonon of the MR. On the contrary, the generation of a Stokes photon will heat the MR by creating a phonon. When the effective detuning  $\Delta > 0$ , the microwave field of the TLR (with the frequency  $\omega_a \equiv \omega_d + \Delta_0 \approx \omega_d + \Delta$ ) interacts with the first anti-Stokes sideband ( $\omega_d + \omega_b$ ) more than it interacts with the first Stokes sideband ( $\omega_d - \omega_b$ ), and cooling will occur. This is the physical reason why the positive effective detuning ( $\Delta > 0$ ) will lead to cooling. In the high-quality cavity limit  $\kappa < \omega_b$ , the anti-Stokes (Stokes) sideband is resolved, and the corresponding cooling (heating) process is prominent. Especially, for the optimal effective

detuning  $\Delta \approx \omega_b$ , the frequency of the TLR is resonant with that of the anti-Stokes sideband, which will apparently lead to optimal cooling. This physical discussion is consistent with the calculation presented above.

Figure 3 suggests there is a finite optimal value of  $\kappa$  for a fixed effective detuning. That is because one should have both a small value of  $n_{ca}$  and a large effective damping rate  $\gamma_{ca}(\omega_b)$  in order to get strong cooling:  $\kappa$  should not be too large, since  $n_{ca}$  depends somewhat on the value of  $\kappa^2/\omega_b^2$ ;  $\kappa$  should not be too small, since  $\gamma_{ca}(\omega_b) \rightarrow 0$  when  $\kappa \rightarrow 0$  [59]. In the cooling process, the thermal energy of the MR is mainly first transferred to the TLR, and then leaks out of the TLR through the bath coupled to the TLR. When the decay rate of the TLR is too small:  $\kappa \rightarrow 0$ , the energy leakage out of the TLR is too weak, and one could not obtain a strong cooling.

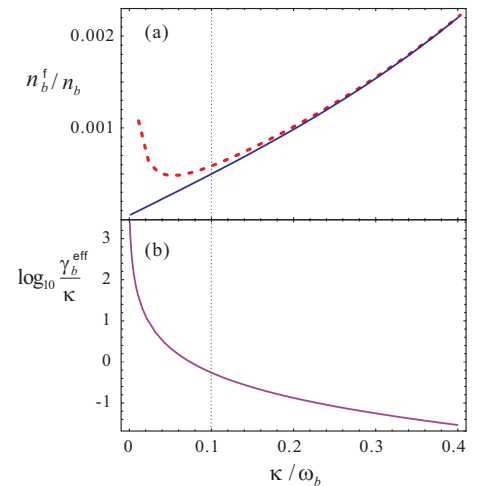


FIG. 4: (Color online) (a) Optimal final mean phonon number obtained by numerically evaluating the integral in Eq. (8) (dashed line) or using the approximate expression in Eqs. (10,13) (solid line) as a function of  $\kappa$  at the optimal effective detuning  $\Delta = \omega_b$ . (b) Logarithm of the ratio of the corresponding effective damping rate  $\gamma_b^{\text{eff}}(\omega_b)$  to  $\kappa$  as a function of  $\kappa$ . Here,  $T = 3 \times 10^3 \hbar\omega_b/k_B$ . For the other parameters see Fig. 2.

We would like to emphasize that the results shown in Fig. 3 are based on the approximate expressions Eqs. (10,13), where the condition of the so-called weak-coupling limit [34, 44] has been assumed, that is, the effective damping rate of the MR should be always less than the decay rate of the cavity and less than the frequency of the MR  $|\gamma_b^{\text{eff}}(\omega_b)| < \kappa, \omega_b$ . Normally the weak-coupling is satisfied but not in some special cases. In Fig. 4(b), the weak-coupling condition is violated when  $\kappa/\omega_b < 0.1$  at the optimal effective detuning  $\Delta = \omega_b$ . Beyond the weak coupling limit, Fig. 4(a) shows that the approximate treatment through Eqs. (10,13) ceases to be valid. Then one should discuss the cooling, e.g., effective mean phonon number in Eq. (7), by using the numerical evaluation of the integral in Eq. (8). But going beyond the weak-coupling limit, the contribution from the posi-

tion variance is not equivalent to that from the momentum variance any more [36]. In other words, the energy equipartition is not satisfied. That means it is hard to define an effective temperature since it is not in a strict thermal state.

According to the above analysis, both the high-quality cavity and weak-coupling limit should be satisfied, so the optimal decay rate of the TLR is better taken to be  $\kappa \approx 0.1\omega_b$  for the typical parameters in Fig. 4. The weak-coupling condition depends only weakly on the initial temperature  $T$  and the original damping rate of the MR  $\gamma_b$  in the cooling process. In what follows, we will consider the optimal decay rate at  $\kappa \approx 0.1\omega_b$  for different parameters  $T$  and  $\gamma_b$ , for which the weak coupling limit is always satisfied.

In Fig. 5, the ratio of final effective temperature  $T_{\text{eff}}$  to bath temperature  $T$  is plotted as a function of the effective detuning  $\Delta$  for the optimal  $\kappa \approx 0.1\omega_b$ . Apparently, here the weak coupling limit is satisfied (according to the above analysis in Fig. 4). For initial temperatures  $T = 100, 30, \text{ and } 10 \text{ mK}$ , the corresponding initial mean phonon numbers are  $n_b = 1/[\exp(\hbar\omega_b/k_B T) - 1] \simeq k_B T/\hbar\omega_b \simeq 3300, 980, \text{ and } 330$ , with the final mean phonon number  $n_b^f \approx 1.6, 0.5, \text{ and } 0.16$ , respectively. It is obvious that a significant cooling of the MR is obtained and lower initial temperatures will generally lead to better cooling. For an initial temperature  $T = 10 \text{ mK}$ , which can be realized experimentally by using a dilution refrigerator, the MR (with the frequency  $\omega_b \sim 4 \text{ MHz}$ ) can be cooled close to the ground state since the final mean phonon number  $n_b^f \approx 0.16 < 1$ .

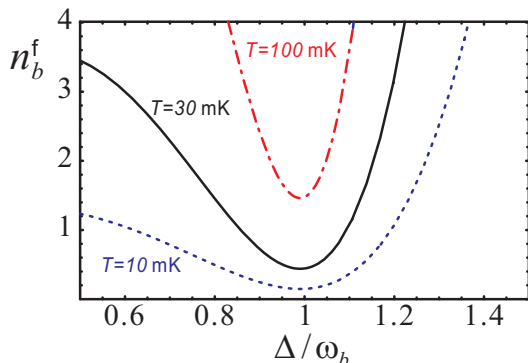


FIG. 5: (Color online) The final mean phonon number vs. effective detuning  $\Delta$  for three initial temperatures:  $T = 10 \text{ mK}$  (dotted lines),  $T = 30 \text{ mK}$  (solid lines),  $T = 100 \text{ mK}$  (dot-dashed lines). Here,  $\kappa = 0.1\omega_b$ ,  $m = 1.5 \times 10^{-13} \text{ kg}$ ,  $\omega_b = 4 \text{ MHz}$ ,  $\gamma_b = 0.25 \times 10^{-4} \omega_b$  (equivalently,  $Q_b \equiv \omega_b/\gamma_b = 4 \times 10^4$ ). For the other parameters see Fig. 2.

For an initial temperature of  $T = 10 \text{ mK}$  as in Fig. 5, the final mean phonon number would in principle be  $n_{ca}$  (in Eq. (16)), which is much less than that obtained in Fig. 5:  $n_{ca} = N + \kappa^2/4\omega_b^2 \approx 0.0025 \ll n_b^f \approx 0.16$ . This is because  $n_b^f \rightarrow n_{ca}$  only when the condition in Eq. (19) is satisfied. Unfortunately, it is not the case for the parameters in Fig. 5. A possible way to approach this condition

is to increase the quality factor of the MR. In Fig. 6, the final effective mean phonon number is plotted as a function of the effective detuning  $\Delta$  for different quality factors of MR  $Q_b (\equiv \omega_b/n_b)$ :  $Q_b = 4 \times 10^4$  (typically, see Ref. [44]);  $Q_b = 10^5, 4 \times 10^5, 10^6$  (expected in the near future). The corresponding minimal  $n_b^f \approx 0.16, 0.06, 0.02, 0.01$ . One can find the cooling is better for a higher quality factor of the MR.

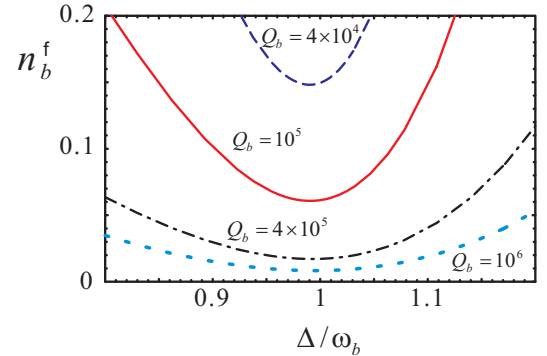


FIG. 6: (Color online) The final effective mean phonon number  $n_b^f$  is plotted as a function of  $\Delta$  for different quality factors of the MR:  $Q_b = 4 \times 10^4, 10^5, 4 \times 10^5, 10^6$  (from up to down), the corresponding damping rate  $\gamma_b = 100, 40, 10, 4 \text{ Hz}$ . Here,  $T = 10 \text{ mK}$ . For the other parameters see Fig. 5.

The cooling discussed above can be measured by a homodyne detection method like that given in the scheme of cavity-assisted radiation-pressure cooling of a MR [32, 44, 47, 61]. The motion of the MR can be detected by monitoring the output microwave signal (e.g., the field phase quadrature) of the TLR (as seen in Fig. 1) since the measurement of the output spectrum corresponds to a faithful measurement of the MR motion [47].

## V. CONCLUSION

We have found that a MR with frequency  $\omega_b \sim 2\pi \times 10^6 \text{ Hz}$  can be cooled close to its ground state when it is coupled to a typical TLR ( $\omega_a \sim 2\pi \times 10^{10} \text{ Hz}$ ). Actually, by considering the optimal parameters in this scheme, that is, assuming the high-quality cavity limit ( $\kappa^2 \ll \omega_b^2$ ), a positive optimal effective detuning ( $\Delta \approx \omega_b$ ), a low initial temperature (e.g.,  $T = 10 \text{ mK}$  in order that  $N \approx 10^{-27} \simeq 0$ ), a high quality factor of the MR ( $Q_b \equiv \omega_b/\gamma_b \gtrsim 10^4$ ), and both strong external input microwave drive power  $P$  and strong capacitive coupling strength  $g_0$  to get the significantly increased positive effective damping rate ( $\gamma_b \ll \gamma_b^{\text{eff}}(\omega_b) \approx \gamma_{ca}(\omega_b)$ ), we find that resolved sideband cooling of the MR occurs. The possible minimal value of the final effective phonon number could approach the induced mean phonon number:  $n_b^f \rightarrow n_{ca} \approx \kappa^2/4\omega_b^2 \ll 1$ . Moreover, one should also consider the condition of weak-coupling limit, that is, the significantly increased effective damping rate  $\gamma_b^{\text{eff}}(\omega_b)$  should be less than both  $\omega_b$  and  $\kappa$  (in the high-quality

cavity limit, one only needs  $\gamma_b^{\text{eff}}(\omega_b) < \kappa$ ). This condition requires that  $\kappa$  must not be too small though lower  $\kappa$  will lead to lower  $n_{ca}$ . As shown in Fig. 2 and its discussion, there will be an optimal range of  $\kappa$ . For the typical parameters in this cooling scheme, we take  $\kappa \sim 0.1\omega_b$  (though this is not the optimal result in general). We find that a MR with  $\omega_b = 4$  MHz can be cooled close to its ground state with the final effective mean phonon number in the steady state:  $n_b^f \approx 0.16$  (for a typical quality factor  $Q_b = 4 \times 10^4$ ) or  $n_b^f \approx 0.01$  (for a high quality factor  $Q_b = 10^6$ ) by using the resolved sideband cooling scheme when it is coupled to a driven TLR (with the frequency  $\omega_a = 8 \times 10^{10}$  Hz).

We would like to stress the condition in Eq. (19), which can lead to  $n_b^f \rightarrow n_{ca}$ . As pointed out in the discussion of Figs. (5, 6), this is not always satisfied. A possible way to approach this condition is to increase the quality factor of the MR. For example, if the quality factor of the MR is high enough (e.g.,  $Q_b > 10^7$ ), one would have the optimal  $n_b^f \rightarrow n_{ca} \approx \kappa^2/4\omega_b^2 = 0.0025$ , for which the MR is cooled much closer to the ground state.

The back-action self-cooling scheme presented here is similar to the optical-cavity-assisted cooling scheme [33, 34]. In both cases, the MR can be cooled close to its ground state using resolved sideband cooling which is possible in the limit of a high-quality cavity. But it seems that this limit (e.g.,  $\kappa = 0.1\omega_b$ , for  $\omega_b = 4 \times 10^6$  Hz) is easier to reach in the microwave TLR than that in the optical cavity. In the case of a TLR (typically  $\omega_a = 8 \times 10^{10}$  Hz), quality factors of  $Q_a = \omega_a/\kappa = 2 \times 10^5$  have been seen in experiments [47, 62]. However, in the case of an optical cavity ( $\omega_a \sim 10^{15}$  Hz), the corresponding quality factor should be  $Q_a = \omega_a/\kappa \sim 2.5 \times 10^9$ , which is hard to achieve since the typical cavity quality factor is  $Q_a \sim 10^{7-8}$  [49].

To conclude, we have studied the self-cooling of a mechanical resonator that is capacitively coupled to a transmission-line resonator. The discussion was based on a linearized quantum Langevin equation. The cooling method presented here is similar to the self-cooling of a MR coupled to an optical cavity by radiation pressure. By using the optimal parameters discussed above, the MR can be cooled close to its ground state in the high-quality cavity and weak-coupling limit.

### Acknowledgments

We would like thank C.B. Doiron and I. Wilson-Rae for helpful discussions. This work was supported by the Swiss NSF, the NCCR Nanoscience, the EC IST-FET project EuroSQUIP, and partially supported by the NSFC through Grant No. 10574133. Y.D.W. also acknowledges support by the JSPS KAKENHI No. 18201018 and MEXT-KAKENHI No. 18001002. F.X. was supported in part at the Technion by an Aly Kaufman Fellowship.

### Appendix A: Equivalence to time-dependent second-order perturbation theory

The linearized quantum Langevin equations read

$$\delta\dot{x} = \delta p/m, \quad (\text{A1a})$$

$$\delta\dot{p} = -m\omega_b^2\delta x - \gamma_b\delta p + \hbar g_0(\delta a^\dagger \langle a \rangle + h.c.) + \xi, \quad (\text{A1b})$$

$$\delta\dot{a} = -(\kappa + i\Delta)\delta a + ig_0 \langle a \rangle \delta x + \sqrt{2\kappa}a_{in}. \quad (\text{A1c})$$

To solve these equations, we define the Fourier transform for an operator  $u$  ( $u = \delta a, \delta x, \delta p, a_{in}, \xi$ )

$$u(t) := \frac{1}{\sqrt{2\pi}} \int_{-\infty}^{+\infty} e^{i\omega t} \tilde{u}(\omega) d\omega, \quad (\text{A2})$$

and for its Hermitian conjugate  $u^\dagger$  (if any)

$$u^\dagger(t) := \frac{1}{\sqrt{2\pi}} \int_{-\infty}^{+\infty} e^{-i\omega t} \tilde{u}^\dagger(\omega) d\omega, \quad (\text{A3})$$

which lead to

$$\langle \tilde{a}_{in}(\Omega) \tilde{a}_{in}^\dagger(\omega) \rangle = (N+1)\delta(\Omega - \omega), \quad (\text{A4})$$

$$\langle \tilde{\xi}(\Omega) \tilde{\xi}(\omega) \rangle = \hbar\gamma_b m\omega (1 + \coth \frac{\hbar\omega}{2k_B T}) \delta(\Omega + \omega). \quad (\text{A5})$$

After solving the linear quantum Langevin equations in the frequency domain, we obtain

$$\delta\tilde{x}(\omega) = \frac{C^*(-\omega)\tilde{a}_{in} + C(\omega)\tilde{a}_{in}^\dagger + [(\kappa + i\omega)^2 + \Delta^2] \tilde{\xi}}{B(\omega)}, \quad (\text{A6a})$$

$$\delta\tilde{p}(\omega) = i\omega m \delta\tilde{x}(\omega), \quad (\text{A6b})$$

where  $B(\omega) = m(\omega_b^2 - \omega^2 + i\gamma_b\omega) [(\kappa + i\omega)^2 + \Delta^2] - 2\hbar|g_0\langle a \rangle|^2\Delta$ , and  $C(\omega) = \hbar\sqrt{2\kappa}g_0\langle a \rangle[\kappa + i(\omega + \Delta)]$ .

To calculate the effective temperature of the MR, we define the fluctuation spectra of position and momentum [32, 36, 51] of the MR, which are given by the following correlation function:

$$S_x(\omega) = \int_{-\infty}^{+\infty} e^{-i\omega\tau} \langle \delta x(t+\tau) \delta x(t) \rangle_s d\tau, \quad (\text{A7})$$

$$S_p(\omega) = \int_{-\infty}^{+\infty} e^{-i\omega\tau} \langle \delta p(t+\tau) \delta p(t) \rangle_s d\tau. \quad (\text{A8})$$

Here,  $\langle \dots \rangle_s$  denotes the steady-state average. Equivalently,  $S_{x,p}(\omega)$  can also be defined as

$$\langle \delta\tilde{r}(\Omega) \delta\tilde{r}(\omega) \rangle_s := S_r(\omega) \delta(\Omega + \omega), \quad (r = x, p). \quad (\text{A9})$$

According to Eqs. (A6), the spectra of the MR can be written as

$$S_x(\omega) \equiv |\chi_{\text{eff}}(\omega)|^2 [S_{th}(\omega) + S_{ca}(\omega)], \quad (\text{A10})$$

$$S_p(\omega) = (\omega m)^2 S_x(\omega), \quad (\text{A11})$$

where

$$S_{th}(\omega) = \hbar\gamma_b m\omega [1 + \coth(\hbar\omega/2k_B T)] \quad (\text{A12})$$

is the thermal noise spectrum due to the Brownian motion of the MR; and

$$\begin{aligned} S_{ca}(\omega) &= \frac{(N+1)|C(\omega)|^2 + N|C(-\omega)|^2}{|(\kappa + i\omega)^2 + \Delta^2|^2} \\ &= 2\hbar^2 |g_0 \langle a \rangle|^2 \kappa \frac{(2N+1)(\kappa^2 + \Delta^2 + \omega^2) + 2\omega\Delta}{|(\kappa + i\omega)^2 + \Delta^2|^2} \end{aligned} \quad (\text{A13})$$

is the induced noise spectrum due to the capacitive coupling to the driven TLR. The effective susceptibility is defined as  $\chi_{\text{eff}}(\omega) = [(\kappa + i\omega)^2 + \Delta^2]^{-1} B(\omega)$  and can be simplified to

$$\chi_{\text{eff}}(\omega) \equiv \frac{1}{m \left[ (\omega_b^{\text{eff}}(\omega))^2 - \omega^2 + i\omega\gamma_b^{\text{eff}}(\omega) \right]}, \quad (\text{A14})$$

where the effective frequency of the MR is

$$\begin{aligned} \omega_b^{\text{eff}}(\omega) &= \sqrt{\omega_b^2 - \frac{2\hbar |g_0 \langle a \rangle|^2 \Delta (\kappa^2 - \omega^2 + \Delta^2)}{m |(\kappa + i\omega)^2 + \Delta^2|^2}} \\ &\equiv \sqrt{\omega_b^2 - \frac{(\kappa^2 - \omega^2 + \Delta^2) \gamma_{ca}(\omega)}{2\kappa}}, \end{aligned} \quad (\text{A15})$$

and the effective damping rate  $\gamma_b^{\text{eff}}(\omega) = \gamma_b + \gamma_{ca}(\omega)$  with the additional term

$$\gamma_{ca}(\omega) = \frac{4\hbar |g_0 \langle a \rangle|^2 \kappa \Delta}{m |(\kappa + i\omega)^2 + \Delta^2|^2} \quad (\text{A16})$$

resulting from the capacitive coupling.

According to the definition of the additional damping rate in Eq. (A16), the induced noise spectrum  $S_{ca}(\omega)$  in Eq. (A13) can also be expressed as

$$S_{ca}(\omega) = m\hbar \left[ (2N+1) \frac{\kappa^2 + \Delta^2 + \omega^2}{2\Delta} + \omega \right] \gamma_{ca}(\omega). \quad (\text{A17})$$

- 
- [1] V. B. Braginsky and A. B. Manukin, *Measurement of Weak Forces in Physics Experiments* (The University of Chicago Press, Chicago, 1977).
- [2] C. M. Caves, K. S. Thorne, R. W. P. Drever, V. D. Sandberg, and M. Zimmermann, *Rev. Mod. Phys.* **52**, 341 (1980); M. F. Bocko and R. Onofrio, *Rev. Mod. Phys.* **68**, 755 (1996); M. D. LaHaye, O. Buu, B. Camarota, and K. C. Schwab, *Science* **304**, 74 (2004).
- [3] K. L. Ekinici, Y. T. Yang, and M. L. Roukes, *J. Appl. Phys.* **95**, 2682 (2004).
- [4] C. M. Caves, *Phys. Rev. Lett.* **45**, 75 (1980).
- [5] B. Abbott *et al.*, *Phys. Rev. Lett.* **95**, 221101 (2005).
- [6] S. Mancini, V. Giovannetti, D. Vitali, and P. Tombesi, *Phys. Rev. Lett.* **88**, 120401 (2002).
- [7] W. Marshall, C. Simon, R. Penrose, and D. Bouwmeester, *Phys. Rev. Lett.* **91**, 130401 (2003).
- [8] J. Eisert, M. B. Plenio, S. Bose, and J. Hartley, *Phys. Rev. Lett.* **93**, 190402 (2004).
- [9] L. F. Wei, Y.-X. Liu, C. P. Sun, and F. Nori, *Phys. Rev. Lett.* **97**, 237201 (2006); X. Hu and F. Nori, *Phys. Rev. Lett.* **76**, 2294 (1996); *ibid* **79**, 4605 (1997).
- [10] F. Xue, L. Zhong, Y. Li, and C. P. Sun, *Phys. Rev. B* **75**, 033407 (2007); F. Xue, Y.-X. Liu, C.P. Sun, and F. Nori, *Phys. Rev. B* **76**, 064305 (2007); F. Xue, Y. D. Wang, C. P. Sun, H. Okamoto, H. Yamaguchi, and K. Semba, *New J. of Phys.* **9**, 35 (2007).
- [11] D. J. Wineland and W. M. Itano, *Phys. Rev. A* **20**, 1521 (1979).
- [12] I. Martin, A. Shnirman, L. Tian, and P. Zoller, *Phys. Rev. B* **69**, 125339 (2004).
- [13] P. Zhang, Y. D. Wang, and C. P. Sun, *Phys. Rev. Lett.* **95**, 097204 (2005).
- [14] J. Hauss, A. Fedorov, C. Hutter, A. Shnirman, and G. Schön, *Phys. Rev. Lett.* **100**, 037003 (2008).
- [15] K. Jaehne, K. Hammerer, and M. Wallquist, arXiv:0804.0603.
- [16] Y. D. Wang, K. Semba, and H. Yamaguchi, *New J. Phys.* **10**, 043015 (2008).
- [17] J. Q. You, Y.-X. Liu, and F. Nori, *Phys. Rev. Lett.* **100**, 047001 (2008).
- [18] A. Naik *et al.*, *Nature* **443**, 193 (2006); M. P. Blencowe, J. Imbers, and A. D. Armour, *New J. Phys.* **7**, 236 (2005); A. A. Clerk and S. Bennett, *ibid* **7**, 238 (2005).
- [19] I. Wilson-Rae, P. Zoller, and A. Imamoglu, *Phys. Rev. Lett.* **92**, 075507 (2004).
- [20] L. Tian and P. Zoller, *Phys. Rev. Lett.* **93**, 266403 (2004).
- [21] C. H. Metzger and K. Karrai, *Nature* **432**, 1002 (2004).
- [22] S. Gigan *et al.*, *Nature* **444**, 67 (2006).
- [23] O. Arcizet, P.-F. Cohadon, T. Briant, M. Pinard, and A. Heidmann, *Nature* **444**, 71 (2006).
- [24] D. Kleckner and D. Bouwmeester, *Nature* **444**, 75 (2006).
- [25] A. Schliesser, P. Del'Haye, N. Nooshi, K. J. Vahala, and T. J. Kippenberg, *Phys. Rev. Lett.* **97**, 243905 (2006).
- [26] T. Corbitt *et al.*, *Phys. Rev. Lett.* **98**, 150802 (2007).
- [27] J. D. Thompson, B. M. Zwickl, A. M. Jayich, F. Marquardt, S. M. Girvin, and J. G. E. Harris, *Nature* **452**, 72 (2008).
- [28] A. Schliesser, R. Rivière, G. Anetsberger, O. Arcizet, and T. J. Kippenberg, *Nature Physics* **4**, 415 (2008).
- [29] S. Mancini, D. Vitali, and P. Tombesi, *Phys. Rev. Lett.* **80**, 688 (1998).
- [30] D. Vitali, S. Mancini, L. Ribichini, and P. Tombesi, *Phys. Rev. A* **65**, 063803 (2002).
- [31] M. Grajcar, S. Ashhab, J. R. Johansson, and F. Nori, *Phys. Rev. B* **78**, 035406 (2008).
- [32] M. Paternostro, S. Gigan, M. S. Kim, F. Blaser, H. R. Böhm, and M. Aspelmeyer, *New J. Phys.* **8**, 107 (2006).
- [33] I. Wilson-Rae, N. Nooshi, W. Zwerger, and T. J. Kippenberg, *Phys. Rev. Lett.* **99**, 093901 (2007).
- [34] F. Marquardt, J. P. Chen, A. A. Clerk, and S. M. Girvin,

- Phys. Rev. Lett. **99**, 093902 (2007).
- [35] M. Bhattacharya and P. Meystre, Phys. Rev. Lett. **99**, 073601 (2007).
- [36] C. Genes, D. Vitali, P. Tombesi, S. Gigan, and M. Aspelmeyer, Phys. Rev. A **77**, 033804 (2008).
- [37] A. Dantan, C. Genes, D. Vitali, and M. Pinard, Phys. Rev. A **77**, 011804(R) (2008).
- [38] T. J. Kippenberg and K. J. Vahala, Optics Express **15**, 17172 (2007).
- [39] F. Marquardt, A. A. Clerk, and S. M. Girvin, arXiv:0803.1164.
- [40] D. J. Wineland *et al.*, arXiv:quant-ph/0606180.
- [41] K. R. Brown, J. Britton, R. J. Epstein, J. Chiaverini, D. Leibfried, and D. J. Wineland, Phys. Rev. Lett. **99**, 137205 (2007).
- [42] F. Xue, Y. D. Wang, Y.-X. Liu, and F. Nori, Phys. Rev. B **76**, 205302 (2007).
- [43] D. Vitali, P. Tombesi, M. J. Woolley, A. C. Doherty, and G. J. Milburn, Phys. Rev. A **76**, 042336 (2007).
- [44] J. D. Teufel, C. A. Regal, and K. W. Lehnert, arXiv:0803.4007.
- [45] M. P. Blencowe and E. Buks, Phys. Rev. B **76**, 014511 (2007).
- [46] E. Buks, S. Zaitsev, E. Segev, B. Abdo, and M. P. Blencowe, Phys. Rev. E **76**, 026217 (2007).
- [47] C. A. Regal, J. D. Teufel, and K. W. Lehnert, Nature Physics **4**, 555 (2008).
- [48] F. Marquardt, Nature Physics **4**, 513 (2008).
- [49] A. Blais, R.-S. Huang, A. Wallraff, S. M. Girvin, and R. J. Schoelkopf, Phys. Rev. A **69**, 062320 (2004).
- [50] Here we assumed the mechanical resonator to be fabricated at the center of the TLR. As a result, the qubit is coupled to the second mode of the TLR, which as an antinode of the voltage in its center as given in Ref. [49].
- [51] C. W. Gardiner and P. Zoller, *Quantum Noise* (Springer-Verlag, Berlin, 2000).
- [52] D. Vitali *et al.*, Phys. Rev. Lett. **98**, 030405 (2007).
- [53] M. Pinard, A. Dantan, D. Vitali, O. Arcizet, T. Briant and A. Heidmann, Europhys. Lett. **72**, 747 (2005).
- [54] Strictly speaking,  $\omega_b^{\text{eff}}(\omega) \simeq \omega_b$  is not always satisfied for arbitrary parameters, but this is the case for the parameters considered in the following discussion.
- [55] A. Hurwitz, *1964 Selected Papers on Mathematical Trends in Control Theory*, Ed. R. Bellman and R. Kalaba (New York: Dover); E. X. DeJesus and C. Kaufman, Phys. Rev. A **35**, 5288 (1987).
- [56] S. D. Bennett and A. A. Clerk, Phys. Rev. B **74**, 201301(R) (2006).
- [57] D.A. Rodrigues, J. Imbers, and A.D. Armour, Phys. Rev. Lett. **98**, 067204 (2007).
- [58] M. Ludwig, B. Kubala, and F. Marquardt, arXiv:0803.3714.
- [59] It is right that  $\gamma_{ca}(\omega_b) \rightarrow 0$  when  $\kappa \rightarrow 0$  except the scope nearly-close to  $\Delta \equiv \omega_b$  where  $\gamma_{ca}(\omega_b) \rightarrow \infty$  when  $\kappa \rightarrow 0$ . But we will show in Fig. 4 that some correction should be done since it may be beyond the weak-coupling limit.
- [60] C. Genes, A. Mari, P. Tombesi, and D. Vitali, arXiv:0806.2045.
- [61] V. Giovannetti and D. Vitali, Phys. Rev. A **63**, 023812 (2001).
- [62] P.K. Day, Henry G. LeDuc, B.A. Mazin, A. Vayonakis, and J. Zmuidzinas, Nature **425**, 817 (2003).